Inhibition impact of synthesized mercapto- and alkylthio-triazole compounds on the corrosion of aluminum in acidic solution

I. Mhaidat,[1] F. Wedian,[1] A.Z. Mifrig[1] and G.M. Al-Mazaideh[2]*

[1]Department of Chemistry, Faculty of Science, Yarmouk University, P.O. Box 560, Irbid, 22163, Jordan
[2]Department of Pharmaceutical Chemistry, College of Pharmacy, University of Hafr Al Batin, P.O. Box 1803, Hafr Al Batin 31991, Saudi Arabia
**E-mail: gmazaideh@uhb.edu.sa*

Abstract

The corrosion inhibition efficiencies (*IE*%) of 5,5-(1,3-phenylene)bis(4-phenyl-4*H*-1,2,4-triazole-3-thiol) (abbreviated as B***M***PTT) and the newly synthesized (bis-1,3-(5-ethylthio-4-phenyl-1,2,4-triazol-3-yl)benzene) (abbreviated as B***E***PTB) on aluminum corrosion in 1.5 M HCl were studied. The structure of the new inhibitors was confirmed by Fourier transform infrared spectroscopy (FTIR), nuclear magnetic resonance (NMR) analysis, and elemental analysis. Electrochemical polarization, weight loss experiments, as well as quantum chemical techniques were employed to study the anticorrosion activity of the new inhibitors. The corrosion monitoring studies revealed that the protection efficiency increased with increasing concentration and temperature. In the temperature range of 25–45°C studied, the *IE*% of B***E***PTB and B***M***PTT varied within 26–78.2% and 16.2–70.8%, respectively. The results revealed that the *IE*% of B***E***PTB was greater than that of B***M***PTT at all concentrations. Furthermore, they showed the potential ability of both compounds to inhibit Al dissolution in acidic media through physisorption; in addition, increasing the temperature enhanced the physical adsorption of molecules at the aluminum surface to form a protective layer. Both inhibitors obeyed Langmuir's adsorption isotherm on the surface of Al during the inhibition process. The inhibitors mainly slowed down the corrosion process by hindering the cathodic reactions. The molecular DFT calculations differentiated the inhibitors' anticorrosion protection powers, which may be attributed to the polarizability of the S atom and the affordability of electron pairs on the N atom in the compounds. An acceptable agreement was observed between the theoretical method and the other corrosion measuring methods.

Received: June 14, 2022. Published: July 30, 2022 doi: 10.17675/2305-6894-2022-11-3-11

Keywords: *corrosion, organic inhibitor, aluminum, triazole, HCl solution.*

Introduction

Aluminum (Al) and its alloys are widely used as materials in several industrial and engineering areas. Aluminum forms a protective adhering oxide film that is stable in dilute solutions of acids [1–3]. Thus, there are many applications that put aluminum and its alloys

in contact with a number of corrosive environments, such as the processes of acid pickling, descaling and cleaning, electroplating, and etching [2, 3].

In acidic media, Al and its alloys quickly react to form ions and/or in some cases, an oxide film [3, 4]. The solubility and stability of the oxide film depends on the acidity of the solution, temperature, and pressure, while its breakdown results in vast economic losses [4]. Although several methods have been developed to prevent the corrosion of Al in industries such as painting, electroplating, anodic/cathodic protection and galvanizing, the use of organic corrosion inhibitors is the most effective and practical method [3–5].

Organic compounds [6], inorganic compounds [7], and polymers [8] were used as corrosion inhibitors for metals in general, and of aluminum and its alloys in particular due to their efficiency in a wide range of temperatures, easy syntheses, good water solubility, low cost, high protection ability, and relatively low toxicity [6–8]. The inhibition efficiency of organic compounds depends on the chemical structure, surface and distribution of charge in the organic molecules, and type of aggressive media [9]. These compounds adsorb on the metal surface through π-electrons of aromatic rings and the heteroatoms in the molecular structure like N, S, O, and P, which serve as active centers for adsorption in acidic solutions. In general, the inhibition efficiency of heteroatoms varies in the order O<N<S<P [9, 10]. Heterocyclic compounds such as azoles, oxadiazoles, thiadiazoles, and triazoles are effective corrosion inhibitors for a wide range of metals and alloys [11–14]. The inhibition process can be attributed to the formation of a protective layer resulting from adsorption of an inhibitor onto a metal, which hinders the corrosion active sites, thus protecting the metal from further attack from the corrosive environment [9, 10].

The quantum chemical techniques are important to explain the absorptive behavior and mechanism of the inhibitory action of various kinds of organic compounds [15]. This work combines the weight loss method, on the one hand, and polarization techniques with quantum chemical techniques, on the other, to investigate for the first time the protection efficiency of new organic inhibitors for aluminum in 1.5 M HCl solution. These inhibitors are the newly synthesized bis-1,3-(5-ethylthio-4-phenyl-1,2,4-triazol-3-yl)benzene (abbreviated as B***E***PTB) and the newly used 5,5-(1,3-phenylene)bis(4-phenyl-*4H*-1,2,4-triazole-3-thiol) (abbreviated as B***M***PTT).

Experimental Details

Chemistry

Isophthalic Acid (98%, Merck), Methanol (99.8%, Mtedia, USA), Sulfuric Acid (98%, Sdfcl), Hydrazine (50–60%, Sigma Aldrich), Ethanol (99.95%, Haymankimia, UK), phenyl-isothiocyanate (98%, Janssen, Geel Belgium), Iodoethane (98%, Sigma-Aldrich), KOH, diethylether, and chloroform (Merck) were used without any purification.

Melting points were tested on an electrothermal-digital apparatus. Nuclear magnetic resonance (NMR) spectra were determined using a Bruker 400 MHz (for ^{1}H) and 100 MHz (for ^{13}C) Avance III spectrometer. The infrared spectral (IR) data were detected on a Bruker

alpha FTIR. The elemental analyses of the elements (C, H and N) were carried out on a Euro EA elemental analyzer 300. Isophthalic dihydrazide **1** and the corresponding B***M***PTT were synthesized according to the reported method [16–18] starting from isophthalic acid.

*Synthesis of bis-1,3-(5-ethylthio-4-phenyl-1,2,4-triazol-3-yl)benzene (B**E**PTB)*

Iodoethane (1.6 g, 0.0103 mole) was added to a solution of potassium hydroxide (KOH) (0.575 g, 0.0103 mols) and B***M***PTT (2.0 g, 0.0047 mole), the mixture was heated under reflux for about 4 hours. After that, the resulting solution was cooled and water was added for precipitation. The resulting white precipitate was collected by filtration and recrystallized from $CHCl_3$/ether.

Yield: 75.0%, m.p. (°C): >250 decomposition, color: white, IR, ν (cm^{-1}): 1510 (C=N), 1321 (C–N), ^{1}H NMR d^6-DMSO (ppm): 7.58–7.54 (m, 6H, Ar),7.31–7.33 (m, 5H, Ar), 7.28–7.26 (m, 3H, Ar), 3.15 (q, 4H, SCH_2), 1.33 (t, 6H, CH_3). ^{13}C NMR (d^6-DMSO) (ppm): 14.48, 26.39, 127, 127.4, 127.5, 128.7, 128.7, 129.9, 130, 133.5, 152.08 and 153.39. Elemental analysis calculated: C: 64.44%, H: 4.99%, N: 17.34%. Formula: $C_{26}H_{24}N_6S_2$, Molecular mass (484.64 g/mol). Found: C: 64.31, H: 4.82, N: 17.27.

Methods

Weight loss experiments

Pure aluminum specimens (99.99% purity, Aldrich) of dimensions 2×2×0.05 cm were used. The specimens were cleaned according to ASTM standard procedure G1-03 (reference). The corrosive 1.50 M HCl solutions were prepared using AR grade reagent and deionized water.

All weight loss measurements were carried out under aerated conditions for the period of experiments in stirred 1.50 M HCl solutions without and with the organic inhibitors at concentrations of 70, 210, 350, and 630 ppm. Specimens were thoroughly washed clean with deionized water, cleaned with acetone, dried, and weighed correctly (accuracy: ±0.1 mg). To evaluate the impact of temperature on the inhibitory power of the organic compounds, all experiments were conducted at 25, 35, and 45°C using a water thermostat. Triple trials were performed and averages were computed.

Electrochemical measurements

A 2.5 cm long Al stem was used as a working electrode for electrochemical polarization measurements. Electrochemical measurements were carried out at steady-state corrosion potential using a three-electrode cell with platinum wire as a counter electrode and an Ag/AgCl reference electrode. The measurements were conducted using a ZRA model Potentiostat/Galvanostat (Gamry instrument, Warminster, PA, USA). Tafel polarization measurements were scanned within ±250 mV with respect to the open circuit potential and scan rate of 10 mV/sec. The corrosion parameters such as corrosion potential (E_{corr}), corrosion current (I_{corr}), anodic and cathodic Tafel slopes (β_a and β_c), and polarization resistance (R_p) were calculated using the Gamry Echem Analyst software.

Computational Details

DFT calculations were carried out using the B3LYP functional with the 631G*(d,p) basis set. The molecules were optimized using DFT-B3LYP and Gaussian 09 (G09) [15]. E_{HOMO}, E_{LUMO}, ΔE_{gap}, the chemical potential (η), global softness (σ), absolute hardness (*X*), fraction of electron transferred (*N*), and electrophilicity index (ω) were the quantum chemical parameters obtained.

Results and Discussion

Characterization

The sequence steps for the synthesis of bis-1,3-(5-mercapto-4-phenyl-4*H*-1,2,4-triazole-3-yl) benzene (B***M***PTT) and (bis-1,3-(5-ethylthio-4-phenyl-1,2,4-triazol-3-yl) benzene) (B***E***PTB) are outlined in Figure 1. The synthesis was started from isophthalic acid. The *IR* spectrum of BEPTT shows peaks at 1510 and 1321 cm^{-1} that correspond to the (C=N) and (C–N) bonds. The ^{1}H NMR spectrum of B***E***PTB shows a quartet peak in the region of 3.13–3.17 ppm and a triplet peak in the region of 1.32–1.34 ppm which are related to $-S\mathbf{CH_2}CH_3$ and $-SCH_2\mathbf{CH_3}$, respectively. The aromatic protons appear in the expected region of δ 7–9 ppm. The ^{13}C NMR spectrum of B***E***PTB is in agreement with the proposed structure. The spectrum shows peaks at 152.1 and 153.4 which are related to C=N carbons and two other signals at 14.48 and 26.39 corresponding to $-SCH_2\mathbf{CH_3}$ and $-S\mathbf{CH_2}CH_3$, respectively.

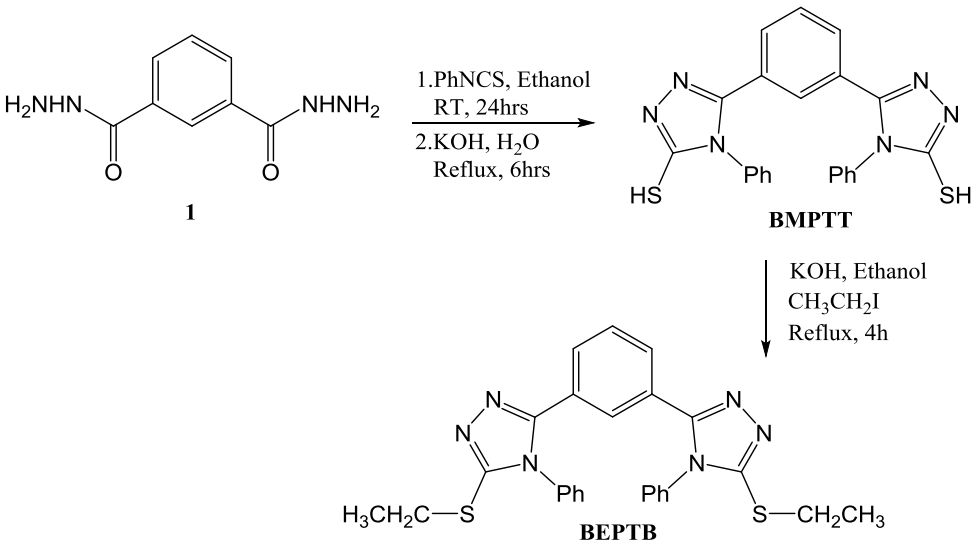

Figure 1. Chemical synthesis of the organic inhibitors B***M***PTT and B***E***PTB.

Mass Loss Studies

The percentage inhibition efficiency (*IE*%) and corrosion rate (*CR*) values computed from weight loss experiments for the corrosion of Al in 1.5 M HCl in the presence of various concentrations of B***E***PTB and B***M***PTT are given in Table 1.

The *IE*% and corrosion rate (*CR*) values were calculated by the following equations [14, 15]:

$$EI\% = \frac{w_0 - w}{w_0} \cdot 100 \quad (1)$$

Corrosion rate (mils per year):

$$CR = \frac{3.45 \cdot 10^6 \cdot w}{A \cdot d \cdot t} \quad (2)$$

where w_0 and w are weight loss of Al in the absence and in the presence of B***E***PTB and B***M***PTT organic inhibitors after time t; A is the surface area of the aluminum specimens (in cm^3); d is the density of aluminum (g/cm^3); t is immersion time (in hours).

Table 1. Corrosion parameters obtained from weight loss measurements for aluminum at contact time 2 h in 1.5 M HCl in the presence of various concentrations of B***E***PTB and B***M***PTT.

Organic inhibitor	Inhibitor concentration (mg/L)	Corrosion rate* mm/year	Inhibition efficiency (*IE*%) at various temperatures		
			25°C	35°C	45°C
B*E*PTB	blank	98.0±5.9	–	–	–
	70	69.1±6.7	26.1	35.3	58.0
	210	56.9±7.0	43.2	51.6	66.6
	350	40.6±6.1	56.5	64.9	74.7
	630	32.5±5.3	63.3	70.9	78.2
B*M*PTT	blank		–	–	–
	70	75.7±7.3	16.2	24.4	48.1
	210	64.0±6.2	33.8	42.9	58.5
	350	52.3±7.0	44.0	51.8	63.4
	630	46.0±6.8	56.3	61.9	70.8

**CR* is the average (millimeter per year)±standard deviation.

Effect of inhibitor concentration

The variation of *IE*% with concentration of B***E***PTB and B***M***PTT at various temperatures is shown in Table 1. Table 1 clearly shows that the inhibition efficiency increases with increasing inhibitor concentrations; moreover, it shows the potential ability of both compounds to inhibit Al dissolution in acidic media. Moreover, at any selected temperature, *IE*% increases with increasing concentration, see Figure 2. Finally, it shows that the inhibition effectiveness of B***E***PTB is higher than that of B***M***PTT in 1.50 M HCl at all

temperatures. The inhibition efficiency values reveal that the chemical structure of inhibitors affects their inhibitive action. This may be due to the alkyl group in B***E***PTB, which is more electron releasing than H in B***M***PTT. As a result, it influences the inhibition action of B***E***PTB and thus reduces the corrosion rate of aluminum. These results agree with a previously published work [14].

The inhibitive efficiencies obtained in this work and previously published values for some triazole derivatives are compared in Table 2. The comparison indicates that the newly used inhibitors offer an acceptable corrosion inhibition in the acidic medium.

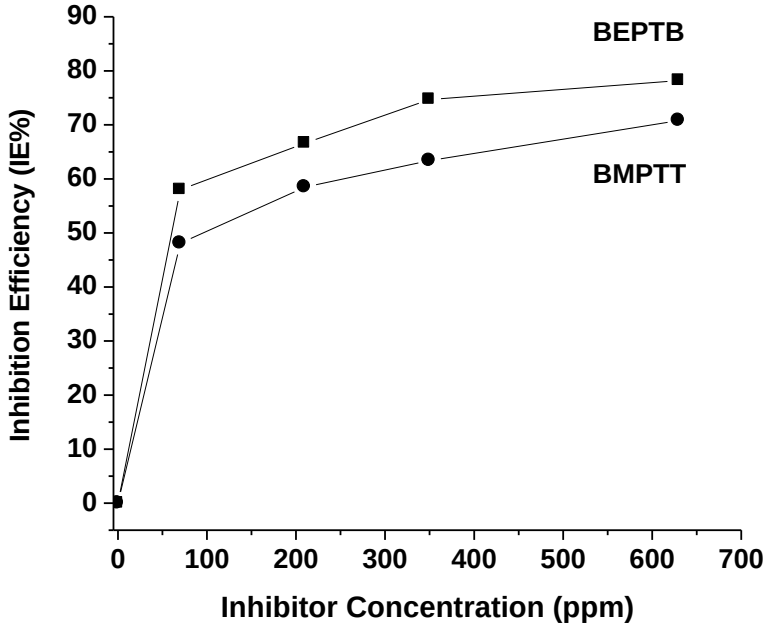

Figure 2. Corrosion inhibition efficiency (*IE*%) of B***E***PTB and B***M***PTT at several concentrations of organic inhibitor, at 45°C.

Table 2. Comparison of selected 1,2,4-triazole derivatives for the corrosion inhibition of various metals and alloys in acid media.

Inhibitor	Concentration	Inhibition efficiency	Metal	Ref.
5,5-(1,3-phenylene)bis(4-phenyl-4*H*-1,2,4-triazole-3-thiol)	650 ppm in 1.5 M HCl	70.8%	aluminum	This work
(bis-1,3-(5-ethylthio-4-phenyl-1,2,4-triazol-3-yl)benzene)	650 ppm in 1.5 M HCl	78.2%	aluminum	This work
(1-ethyl-7-methyl-3-(4-methyl-5-((4-methylbenzyl)thio)-4*H*-1,2,4-triazol-3-yl)-1,8-naphthyridin-4(1*H*)-one)	650 ppm in 1.5 M HCl	84.1%	aluminum	15
ethyl 2-(4-phenyl-1*H*-1,2,3-triazol-1-yl)acetate [Tria-CO_2Et]	$1 \cdot 10^{-3}$ M in 1.0 M HCl	95%	mild steel	19

Inhibitor	Concentration	Inhibition efficiency	Metal	Ref.
2-(4-phenyl-1*H*-1,2,3-triazol-1-yl) acetohydrazide [Tria-CONHNH$_2$]	$1 \cdot 10^{-3}$ M in 1.0 M HCl	95.3%	mild steel	19
1-(6-(4-nitrophenyl)-7*H*[1,2,4]triazolo[3,4-b], [1,3,4]thiadiazine3-yl)ethanol	0.25 mmol in 1.0 M HCl	68.74%	mild steel	20
5-Amino-3-mercapto-1,2,4-triazole	$1 \cdot 10^{-2}$ M in 0.10 M HCl	92%	mild steel	21
3,5-Bis(2-thienylmethyl)-4-amino-1,2,4-triazole	$5 \cdot 10^{-6}$ M in 1.0 M HCl	79.5%	carbon steel	22
1,3-bis((1-benzyl-1H-1,2,3-triazol-4-yl) methyl)pyrimidine-2,4(1H,3H)-dione	200 ppm in 1.0 M HCl	92%	mild steel	23
4-amino-3-ethyl-5-mercapto-1,2,4-triazole	$2.58 \cdot 10^{-3}$ M in 0.5 M HCl	96.09%	copper	24
3,5-bis(4-(methylthio)phenyl)-4*H*-1,2,4-triazole	$5.0 \cdot 10^{-4}$ M in 1.0 M HCl	99%	mild steel	25
3-phenyl-4-amino-5-mercapto-1,2,4-triazole	$1 \cdot 10^{-3}$ M in 2.0 M H_3PO_4	97%	mild steel	26

Effect of Temperature

The variation of *IE*% with temperature is found in Figure 3. It implies that increasing the temperature led to an increase in inhibition efficiency in the presence of both inhibitors. This offers that the inhibitive action of B***E***PTB and B***M***PTT is through physisorption; in addition, elevating the temperature enhances the adsorption of molecules at the aluminum surface to form a protective layer [27]. At any selected temperature, the *IE*% stands in the order B***E***PTB>B***M***PTT.

Potentiodynamic Polarization (Tafel) Studies

The results of potentiodynamic polarization of aluminum in 1.5 M HCl at different concentrations of inhibitors are presented in Figure 4. Table 3 provides information about the corrosion potential (E_{corr}), corrosion current density (I_{corr}), cathodic Tafel slope (β_c), anodic Tafel slope (β_a), as well as percentage inhibition efficiency (*IE*%). The *IE*% was calculated using Equation (3) [15]:

$$IE\% = \frac{I_{corr}^0 - I_{corr}}{I_{corr}^0} \cdot 100 \quad (3)$$

where I_{corr}^0 and I_{corr} are the corrosion current densities in the absence and in the presence of an inhibitor, respectively. Figure 3 shows the Tafel plots produced after two hours of contact with 1.5 M HCl for B***E***PTB and B***M***PTT. The corrosion current density I_{corr} was found to

decrease with an increase in concentrations of both inhibitors, while B***E***PTB was a more efficient inhibitor than B***M***PTT. In addition, E_{corr} shifted negatively for both inhibitors and ΔE_{corr} values were lower than 85 mV with respect to E_{corr} of uninhibited solution. Moreover, the values of anodic slopes β_a remained almost constant with addition of the inhibitors, unlike the cathodic slopes β_c which increased more considerably, suggesting that the inhibitor molecules are adsorbed more strongly on the cathodic sites [28]. These results suggest that B***E***PTB and B***M***PTT act as mixed-type inhibitors with a predominant effect on the cathodic reactions, resulting in the inhibition of both aluminum dissolution and the cathodic reaction of hydrogen evolution.

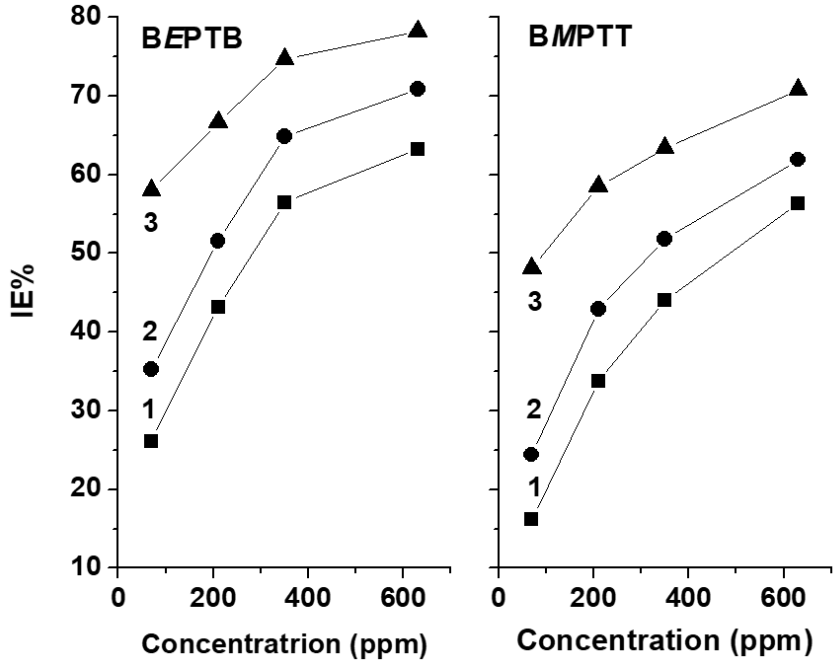

Figure 3. Inhibition efficiency *IE*% at different temperatures: (A) B***E***PTB and (B) B***M***PTT in 1.5 M HCl in the presence of various concentrations of organic inhibitors; 1: 25°C; 2: 35°C; 3: 45°C.

Table 3. Electrochemical parameters and corrosion inhibition efficiency of aluminum in 1.50 M HCl in the presence of various concentrations of B***E***PTB and B***M***PTT.

Inhibitor	**Conc. (ppm)**	E_{corr} **(V/SCE)**	β_a **(mV/dec)**	β_b **(mV/dec)**	R_p **(Ω·cm²)**	I_{corr} **(μA/cm²)**	***IE*** **(%)**
	Blank	–0.788	40.9	75.4	49.6	184.3	–
B***E***PTB	70	–0.794	33.1	81.9	138.4	73.9	60.0
	210	–0.800	55.5	229.1	412.3	28.1	84.7
	350	–0.810	39.0	255.0	763.1	19.3	89.5
	630	–0.822	51.7	309.3	1298.2	14.9	91.8

Inhibitor	Conc. (ppm)	E_{corr} (V/SCE)	β_a (mV/dec)	β_b (mV/dec)	R_p ($\Omega \cdot cm^2$)	I_{corr} ($\mu A/cm^2$)	*IE* (%)
B*M*PTT	70	–0.794	60.9	42.6	129.7	84.0	53.0
	210	–0.800	58.2	76.6	380.5	36.7	79.4
	350	–0.804	61.3	194.1	743.5	27.2	84.8
	630	–0.816	64.4	236.3	972.0	22.8	87.2

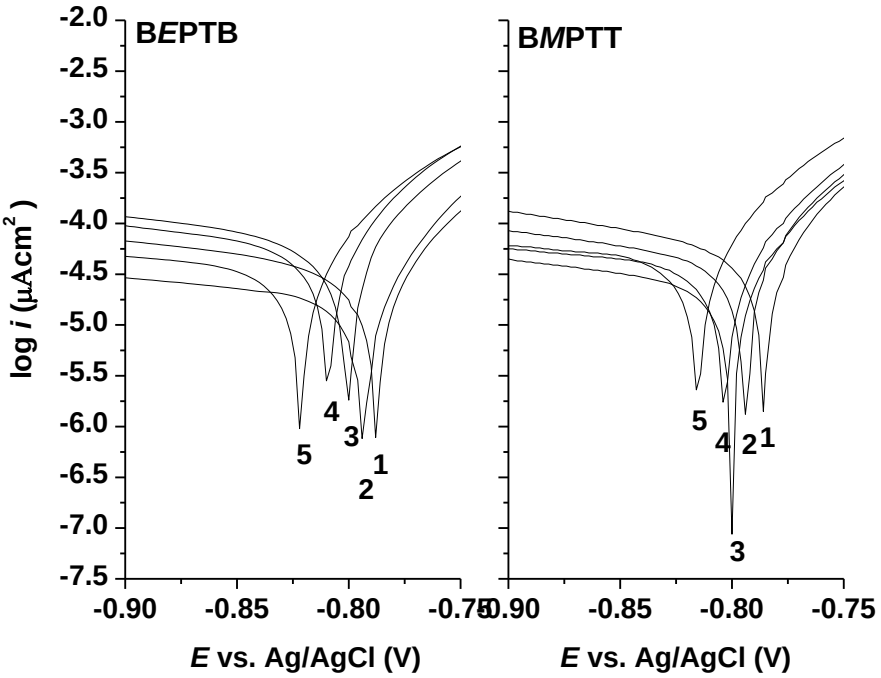

Figure 4. Potentiodynamic polarization of aluminum in 1.50 M HCl at various concentrations of B*E*PTB and B*M*PTT inhibitors at 25°C. 1: blank, 2: 70 ppm, 3: 210 ppm, 4: 350 ppm, 5: 630 ppm.

The inhibition efficiencies increase with increasing the concentration of both inhibitors and reach 91 and 87% for B*E*PTB and B*M*PTT, respectively. This indicates that the synthesized inhibitors adsorb onto the surface and block the reaction active sites on the aluminum surface by forming a barrier layer that limits the interaction of aluminum with the corrosive medium and thus prevents aluminum from corroding [28, 29].

Adsorption isotherm

The adsorption isotherm can provide information about the interaction between the inhibitors and aluminum surface. The nature of interaction between the Al surface and inhibitors can be better understood in terms of the adsorption isotherm [28, 29]. The best adsorption isotherm model that describes the phenomenon was the Langmuir model, as seen in Figure 5.

The formula of the Langmuir model used to describe the adsorption of inhibitor is given by Equation (4) [29]:

$$\frac{C_{\text{inh}}}{\theta} = \frac{1}{K_{\text{ads}}} + C_{\text{inh}} \tag{4}$$

where θ is the degree of surface coverage which is identified as (*IE*%)/100 (see Table 1), *C* is the concentration of inhibitors, and K_{ads} is the equilibrium constant of the adsorption process. The plot of C_{inh}/θ against C_{inh} as in Figure 5 yields a straight line with a slope close to unity [29]. The K_{ads} can be computed from the straight-line intercept on the C_{inh}/θ axis. It was used to determine the standard free energy of adsorption (ΔG^0_{ads}) as follows in Equation (5):

$$\Delta G^0_{\text{ads}} = -RT \ln\left(1 \cdot 10^6 K_{\text{ads}}\right) \tag{5}$$

where *R* is the gas constant (8.314 $\text{J} \cdot \text{K}^{-1} \cdot \text{mol}^{-1}$), *T* is the absolute temperature (K), and $1 \cdot 10^6$ is the concentration of water in $\text{mg} \cdot \text{L}^{-1}$ [28]. The K_{ads} and ΔG^0_{ads} values are tabulated for B***E***PTB and B***M***PTT, see Table 4. The B***E***PTB and B***M***PTT inhibitors get spontaneously adsorbed on Al surface, and the layer being stable is indicated by the negative values of the standard free energy of adsorption.

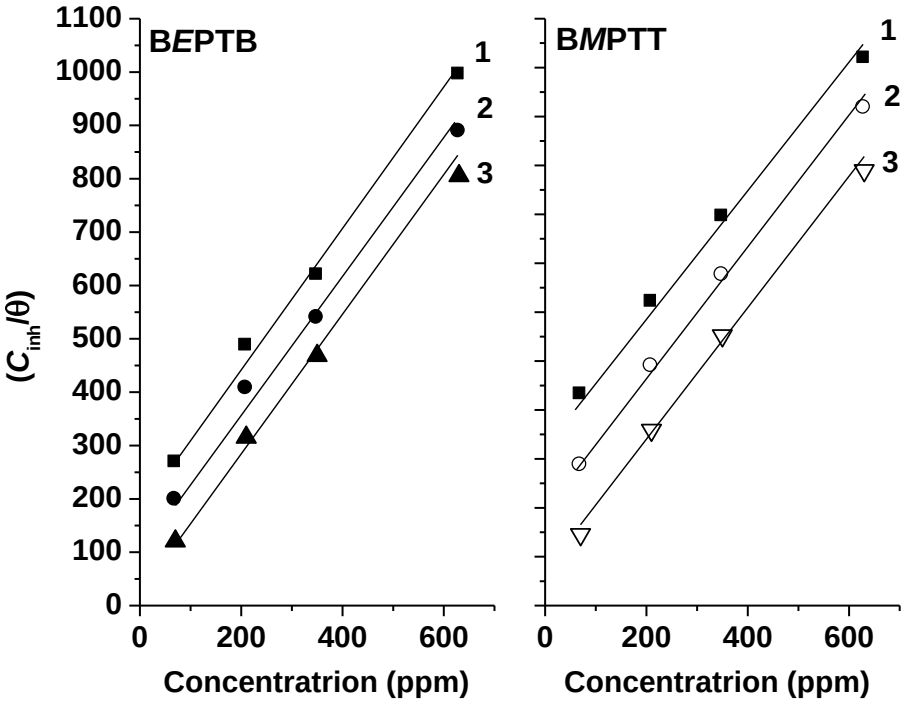

Figure 5. Langmuir's adsorption isotherm of the synthesized organic inhibitors on the Al surface in 1.5 M HCl at 2 h contact time and various temperatures: 1: 25°C, 2: 35°C, and 3: 45°C.

In this study, negative values of ΔG^0_{ads} and high K_{ads} are observed in the order B***E***PTB>B***M***PTT, implying that B***E***PTB is more efficient than B***M***PTT in 1.50 M HCl [28]. In our study, the calculated value of ΔG^0_{ads} ($-24\ kJ \cdot mol^{-1}$) indicates that the adsorption mechanism of B***E***PTB and B***M***PTT onto Al surface is a physical adsorption process [29]; the *IE*% of both inhibitors is less than 80% which means that the layer is incomplete due to the bulkiness of the inhibitors.

Table 4. The adsorption parameters of B***E***PTB and B***M***PTT on aluminum in 1.5 M HCl at different temperatures.

Corrosion Inhibitor	Temperature, K	K_{abs} / ppm^{-1}	ΔG^0_{ads} (kJ·mol^{-1})
B***E***PTB	298	$5.22 \cdot 10^{-3}$	–21.20
	308	$7.87 \cdot 10^{-3}$	–22.60
	318	$2.15 \cdot 10^{-2}$	–26.31
B***M***PTT	298	$2.80 \cdot 10^{-3}$	–19.67
	308	$4.79 \cdot 10^{-3}$	–21.70
	318	$1.41 \cdot 10^{-2}$	–25.26

Computational Works

The adsorption efficiency of molecules on metallic surface and their chemical reactivity are described by the Frontier Molecular Orbital Theory (FMO), which reflects the correlation between the HOMO (Highest Occupied Molecular Orbitals) as well as LUMO (Lowest Unoccupied Molecular Orbitals) molecular orbital levels [30]. Theoretical DFT was used to calculate the two active compounds with the abbreviated names B***E***PTB and B***M***PTT. The optimal geometry of these compounds and their molecular orbitals, HOMO and LUMO, are shown in Figure 6.

The energy separation indicated by the HOMO–LUMO gap (as related to the ΔE_{gap}) suggests a molecular reaction toward metal surface adsorption. As the ΔE_{gap} decreases, the inhibitor reactivity and efficiency will increase [31, 32]. Furthermore, E_{gap} defines the "softness" and "global hardness" values. A soft molecule has larger and relatively polarizable atoms that can work as donor atoms [33–35]. The quantum chemical and molecular dynamic characteristics of energy division (ΔE_{gap}), global hardness (η), softness (σ), chemical potentials (χ), electron fraction transmitted (ΔN), and electrophilicity index (ω) of B***E***PTB and BMPTB were calculated (Table 5).

The ΔE_{gap} of the studied compounds increases in the following order: B***E***PTB>B***M***PTT. B***M***PTT has the highest softness (σ) and the lowest global hardness (η). Furthermore, when compared to B***E***PTB, B***M***PTT has the highest electrophilicity index (ω) value. ω represents an inhibitor's ability to accept electrons from metal surfaces [36]. B***E***PTB has high capacity to accept electrons from Al which is indicated by the

E_{LUMO} (−1.431 eV). Furthermore, when compared to B***M***PTT, the fraction of transferred electrons (ΔN) shows that most electrons transferred to the Al surface come from B***E***PTB molecules (N=0.067). When N is less than 3.6, the inhibition efficiency of most organic inhibitors increases with increasing electron donating ability at the meal surface [36, 37].

	B*M*PTT	**B*E*PTB**
Chemical structure	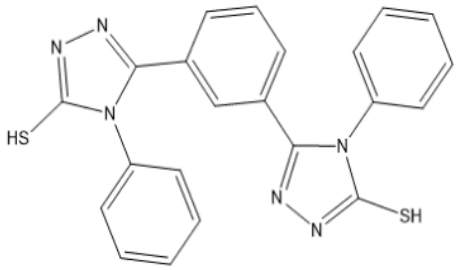	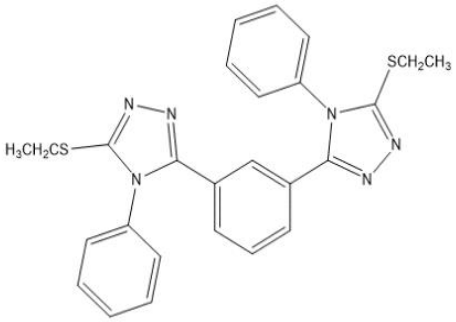
Optimized structure	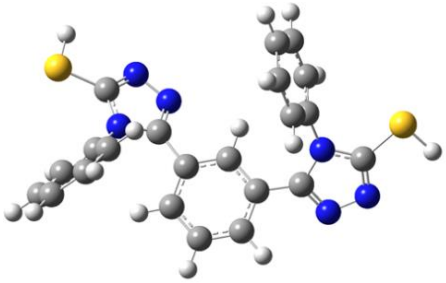	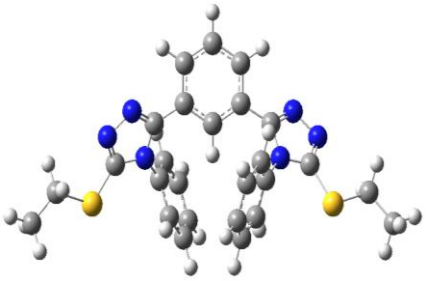
HOMO	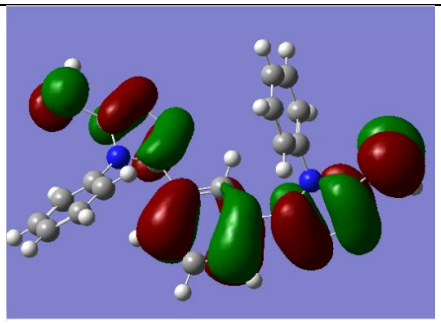	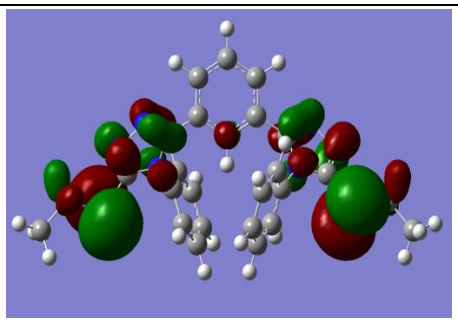
LUMO	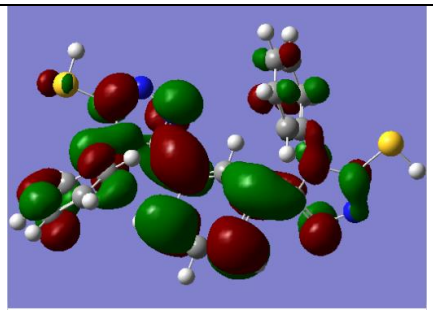	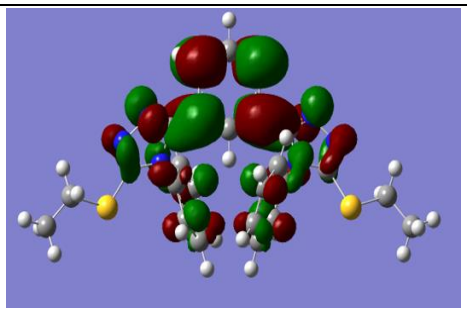

Figure 6. DFT calculated HOMO and LUMO of B***E***PTB and B***M***PTT (Blue: N, Yellow: S, Gray: C, and White: H).

Table 5. DFT quantum parameters of B***E***PTB and B***M***PTT.

	B*E*PTB		**B*M*PTT**	
	Gas	**Aqueous**	**Gas**	**Aqueous**
E_{HOMO} (eV)	–5.861	–6.348	–5.957	–6.174
E_{LUMO} (eV)	–1.176	–1.589	–1.431	–1.525
ΔE_{gap} (eV)	4.685	4.759	4.526	4.649
σ	0.427	0.420	0.441	0.430
η	2.342	2.380	2.263	2.325
χ	3.519	3.969	3.694	3.850
ω	2.198	2.164	2.275	2.215
ΔN	0.030	0.074	0.048	0.063
μ (Debye)	6.678	9.711	5.043	6.521

χ_{Al}=3.209 eV; η_{Al}=2.776 [34].

Mechanism of inhibition

The appearance of heteroatoms of sulfur, nitrogen, and π-electrons of aromatic rings is thought to be responsible for B***E***PTB and B***M***PTT adsorption [38]. The findings suggest that B***E***PTB as well as B***M***PTT can adsorb on the surface through electron donation from electron-rich centers towards the Al surface's vacant d-orbitals, as well as by accepting electrons from Al surface, beginning to form a back-donating bond that is dependent on the orientation of the inhibitor's structural parameters in the gas phase.

The findings suggest that the B***E***PTB molecule has the best ability to adsorb on the Al surface by donating an unshared pair of electrons from the N and S atoms to the Al surface's vacant d-orbitals. In an acidic medium, there are two types of inhibitor adsorption on the aluminum surface: physisorption and chemisorption. The difference in chemical potential between Al metal and the inhibitors determines the magnitude of adsorption. The calculated ΔG_{ads} values of B***E***PTB and B***M***PTT are –19.690 and –16.829 kJ·mol^{-1}, respectively. Since ΔG_{ads} values range between 0 and –40 kJ·mol^{-1}, the mechanism of inhibitor adsorption appears to be a spontaneous physical adsorption.

Conclusion

For the first time, the novel organic compounds (B***E***PTB and B***M***PTT) were synthesized and tested as corrosion inhibitors on the surface of Al in 1.5 M HCl solutions at 25, 35, and 45°C. The inhibitive processes of these compounds were found to be affected by the presence of heteroatoms and the type of substituent. B***E***PTB and B***M***PTT were found to be effective inhibitors, with their inhibition efficiency increasing with increasing concentration and temperature. B***E***PTB and B***M***PTT had the maximum inhibition efficiencies of 91 and 87%,

respectively. The inhibitors primarily slowed corrosion by preventing the cathodic reaction. FMO revealed that both molecules have an inhibitive strength, with B***E***PTB having a higher inhibition efficiency than B***M***PTT, which may be attributed to the polarizability of the S atom and the affordability of electron pairs on the N atom in the compounds.

Acknowledgements

The authors acknowledge the financial support from the Deanship of Scientific Research and Graduate Studies, Yarmouk University.

Conflict of interest

The authors have no conflicts of interest to declare that are relevant to the content of this article.

References

1. M. Jacques, *Corrosion of aluminium*, ISBN, France, 2004.
2. J. Zhao, L. Xia, A. Sehgal, D. Lu, R.L. McCreery and G.S. Frankel, Effects of chromate and chromate conversion coatings on corrosion of aluminium alloy 2024-T3, *Surf. Coat. Technol*., 2001, **140**, no. 1, 51–57. doi: 10.1016/S0257-8972(01)01003-9
3. W.W. Binger, P.L. Laque and M.R. Copson, *Corrosion Resistance of Metals and Alloys*, Reinhold Publishing Corp.: New York, NY, USA, 1963.
4. V. Branzoi, F. Golgovici, and F. Branzoi, Aluminium corrosion in hydrochloric acid solutions and the effect of some organic inhibitors, *Mater. Chem. Phys*., 2003, **78**, no. 1, 122–131. doi: 10.1016/S0254-0584(02)00222-5
5. O.E. Nnabuk, Y.H. Momoh and E.E. Oguzie, Theoretical and experimental studies on the corrosion inhibition potentials of some purines for aluminium in 0.1 M HCl, *J. Adv. Res*., 2015, **6**, no. 2, 203–217. doi: 10.1016/j.jare.2014.01.004
6. H.L. Wang, H.B. Fan and J.S. Zheng, Corrosion inhibition of mild steel in hydrochloric acid solution by a mercapto-triazole compound, *Mater. Chem. Phys*., 2003 ,**77**, no. 3, 655–661. doi: 10.1016/S0254-0584(02)00123-2
7. B. Muller and S. Fisher, Epoxy ester resins as corrosion inhibitors for aluminium and zinc pigments, *Corros. Sci*., 2006, **48**, no. 9, 2406–2416. doi: 10.1016/j.corsci.2005.10.002
8. M.A. Arenos, M. Bethencourt, F.G. Botana, J. Domborenena and M. Marcos, Inhibition of 5083 Aluminium alloy and Galvanised Steel by Lanthanide Salts, *Corros. Sci*., 2001, **43**, no. 1, 157–170. doi: 10.1016/S0010-938X(00)00051-2
9. M.A. Amin, O.A. Hazzazi, S.S. Abd El-Rhim, E.F. El-Sherbini and M.N. Abbas, Polyacrylic Acid as A Corrosion Inhibitor for Aluminium in Weakly Alkaline Solutions. Part I: Weight Loss, Polarization, Impedance EFM and EDX Studies, *Corros. Sci*., 2009, **51**, no. 3, 658–667. doi: 10.1016/j.corsci.2008.12.008

10. G. Sığırcık, T. Tüken and M. Erbil, Assessment of the inhibition efficiency of 3,4-diaminobenzonitrile against the corrosion of steel, *Corros. Sci*., 2016, **102**, 437–445. doi: 10.1016/j.corsci.2015.10.036
11. N. Kıcır, G. Tansuğ, M. Erbil and T. Tüken, Investigation of ammonium (2,4-dimethylphenyl)-dithiocarbamate as a new, effective corrosion inhibitor for mild steel, *Corros. Sci*., 2016, **105**, 88–99. doi: 10.1016/j.corsci.2016.01.006
12. M. Abdallah, E.A.M. Gad, J.H. Al-Fahemi and M. Sobhi, Experimental and Theoretical Investigation by DFT on the Some Azole Antifungal Drugs as Green Corrosion Inhibitors for Aluminum in 1.0 M HCl, *Prot. Met. Phys. Chem. Surf*., 2018, **54**, 503–512. doi: 10.1134/S207020511803022X
13. O.A. Hazazi and M. Abdallah, Investigation of the Corrosion Resistance of some Safely Additives and Mixed Salts – Scales on S41000 Stainless Steel Surface in Synthetic Seawater, *Int. J. Electrochem. Sci*., 2013, **8**, no. 6, 8126–8137.
14. A.Y. Musa, A.A.H. Kadhum, A.B. Mohamad, M.S. Takriff and E.P. Chee, Inhibition of aluminum corrosion by phthalazinone and synergistic effect of halide ion in 1.0 M HCl, *Curr. Appl. Phys*., 2012, **12**, no. 1, 325–330. doi: 10.1016/j.cap.2011.07.001
15. F. Wedian, I. Mhaidat, N.A. Braik and G.M. Al-Mazaideh, A corrosion inhibitor for aluminum by novel synthesized triazole compounds in basic medium, *Int. J. Corros. Scale Inhib*., 2022, **11**, no. 1, 364–381. doi: 10.17675/2305-6894-2022-11-1-22
16. A.H. Frazer and F.T. Wallenberger, Aromatic polyhydrazides: A new class of highly bonded, stiff polymers, *J. Polym. Sci*., *Part A: Gen. Pap*., 1964, **2**, no. 3, 1147–1156. doi: 10.1002/pol.1964.100020312
17. A. Mobinikhaledi, N. Foroughifar and A. Rafiee, Synthesis of some novel bis-1,2,4-triazole and bis-1,3,4-thiadiazole derivatives from terephthaloyl and isophthaloyl chlorides, *Heterocycl. Commun*., 2013, **19**, no. 4, 265–269. doi: 10.1515/hc-2013-0035
18. M. Shkoor, H. Tashtoush, M. Al-Talib, I. Mhaidat, Y. Al-Hiari, V. Kasabri and S. Alalawi, Synthesis and Antiproliferative and Antilipolytic Activities of a Series of 1,3- and 1,4-Bis[5-(R-sulfanyl)- 1,2,4-triazol-3-yl)benzenes, *Russ. J. Org. Chem*., 2021, **57**, 1141–1151. doi: 10.1134/S1070428021070149
19. A. Nahlé, R. Salim, F. El Hajjaji, M.R. Aouad, M. Messali, E. Ech-chihbi, B. Hammouti and M. Taleb, Novel triazole derivatives as ecological corrosion inhibitors for mild steel in 1.0 M HCl: experimental & theoretical approach, *RSC Adv*., 2021, **11**, no. 7, 4147–4162. doi: 10.1039/D0RA09679B
20. N. Arshad, A.R. Akram, M. Akram and I. Rasheed, Triazolothiadiazine derivatives as corrosion inhibitors for copper, mild steel and aluminum surfaces: electrochemical and quantum investigations, *Prot. Met. Phys. Chem. Surf*., 2017, **53**, 343–358. doi: 10.1134/S2070205117020046
21. H.H. Hassan, E. Abdelghani and M.A. Amin, Inhibition of mild steel corrosion in hydrochloric acid solution by triazole derivatives: Part I. Polarization and EIS studies, *Electrochim. Acta*, 2007, **52**, no. 22, 6359–6366. doi: 10.1016/j.electacta.2007.04.046

22. M. Tourabi, K. Nohair, M. Traisnel, C. Jama and F. Bentiss, Electrochemical and XPS studies of the corrosion inhibition of carbon steel in hydrochloric acid pickling solutions by 3,5-bis(2-thienylmethyl)-4-amino-1,2,4-triazole, *Corros. Sci*., 2013, **75**, 123–133. doi: 10.1016/j.corsci.2013.05.023
23. A. Espinoza-Vázquez, G.E. Negrón-Silva, R. González-Olvera, D. Angeles-Beltrán, H. Herrera-Hernández, M. Romero-Romo and M. Palomar-Pardavé, Mild steel corrosion inhibition in HCl by di-alkyl and di-1,2,3-triazole derivatives of uracil and thymine, *Mater. Chem. Phys*., 2014, **145**, no. 3, 407–417. doi: 10.1016/j.matchemphys.2014.02.029
24. E.G. Demissie, S.B. Kassa and G.W. Woyessa, Quantum chemical study on corrosion inhibition efficiency of 4-amino-5-mercapto-1,2,4-triazole derivatives for copper in HCl solution, *Int. J. Sci. Eng. Res*., 2014, **5**, no. 6, 304–312.
25. F. Bentiss, M. Bouanis, B. Mernari, M. Traisnel, H. Vezin and M. Lagrenée, Understanding the adsorption of 4H-1,2,4-triazole derivatives on mild steel surface in molar hydrochloric acid, Appl. Surf. Sci., 2007, **253**, no. 7, 3696–3704. doi: 10.1016/j.apsusc.2006.08.001
26. L. Wang, M.J. Zhu, F.C. Yang and C.W. Gao, Study of a Triazole Derivative as Corrosion Inhibitor for Mild Steel in Phosphoric Acid Solution, *Int. J. Corros*., 2012, **2012**, 1–6. doi: 10.1155/2012/573964
27. S.A. Umoren, E.E. Ebenso and O. Ogbobe, Synergistic effect of halide ions and polyethylene glycol on the corrosion inhibition of aluminium in alkaline medium, *J. Appl. Polym. Sci*., 2009, **113**, no. 6, 3533–3543. doi: 10.1002/app.30258
28. S.A. Refaey, F. Taha and A.M. Abd El-Malak, Corrosion and inhibition of 316L stainless steel in neutral medium by 2-Mercaptobenzimidazole, *Int. J. Electrochem. Sci*., 2006, **1**, 80–91. doi: 10.20964/1020080
29. E. Ituen, O. Akaranta and A. James, Evaluation of performance of corrosion inhibitors using adsorption isotherm models: an overview, *Chem. Sci. Int. J*., 2017, **18**, no. 1, 1–34. doi: 10.9734/CSJI/2017/28976
30. E. Ech-Chihbi, M.E. Belghiti, R. Salim, H. Oudda, M. Taleb, N. Benchat, B. Hammouti and F. El-Hajjaji, Experimental and computational studies on the inhibition performance of the organic compound "2-phenylimidazo [1, 2-a] pyrimidine-3-carbaldehyde" against the corrosion of carbon steel in 1.0 M HCl solution, *Surf. Interfaces*, 2017, **9**, 206–217. doi: 10.1016/j.surfin.2017.09.012
31. D.F. Lewis, C. Ioannides and D.V. Parke, Interaction of a series of nitriles with the alcohol-inducible isoform of P450: computer analysis of structure-activity relationships, *Xenobiotica*, 1994, **24**, no. 5, 401–408. doi: 10.3109/00498259409043243
32. C.U. Ibeji, I.A. Adejoro and B.B. Adeleke, A Benchmark Study on the Properties of Unsubstituted and Some Substituted Polypyrroles, *J. Phys. Chem. Biophys*., 2015, **5**, no. 6, 1–11. doi: 10.4172/2161-0398.1000193

33. Z. Zhou and R.G. Parr, Activation hardness: new index for describing the orientation of electrophilic aromatic substitution, *J. Am. Chem. Soc*., 1990, **112**, no. 15, 5720–5724. doi: 10.1021/ja00171a007
34. R.G. Pearson, Absolute electronegativity and hardness: application to inorganic chemistry, *Inorg. Chem*., 1988, **27**, no. 4, 734–740. doi: 10.1021/IC00277A030
35. R.G. Pearson, Absolute electronegativity and hardness: applications to organic chemistry, *J. Org. Chem*., 1989, **54**, no. 6, 1423–1430. doi: 10.1021/jo00267a034
36. A.S. Fouda, K. Shalabi and A.A. Idress, *Ceratonia siliqua extract* as a green corrosion inhibitor for copper and brass in nitric acid solutions, *Green Chem. Lett. Rev*., 2015, **8**, 17–29. doi: 10.1080/17518253.2015.1073797
37. J. Fang and J. Li, Quantum chemistry study on the relationship between molecular structure and corrosion inhibition efficiency of amides, *J. Mol. Struct.: THEOCHEM*, 2002, **593**, no. 1–3, 179–185. doi: 10.1016/S0166-1280(02)00316-0
38. Y.C. Wu, P. Zhang, H.W. Pickering and D.L. Allara, Effect of KI on improving copper corrosion inhibition efficiency of benzotriazole in sulfuric acid electrolytes, *J. Electrochem. Soc*., 1993, **140**, 2791–2800. doi: 10.1149/1.2220912

♦ ♦ ♦